

# *Special Issue on Chemistry*

## **Green Synthesis of Nickel Aluminate ( $\text{NiAl}_2\text{O}_4$ ) Nanoparticles using the Plant Extract of *Pedaliump murex***

C. Arunkumar and A. Manikandan

*Issue Editor*  
**Dr. A. Manikandan**

Research Journal of Agricultural Sciences  
An International Journal

P- ISSN: 0976-1675  
E- ISSN: 2249-4538

Volume: 13  
Issue: Special

*Res. Jr. of Agril. Sci. (2022) 13(S): 099–102*



# Green Synthesis of Nickel Aluminate ( $\text{NiAl}_2\text{O}_4$ ) Nanoparticles using the Plant Extract of *Pedaliium murex*

C. Arunkumar<sup>1</sup> and A. Manikandan\*<sup>2</sup>

Received: 10 Dec 2021 | Revised accepted: 18 Feb 2022 | Published online: 25 Feb 2022

© CARAS (Centre for Advanced Research in Agricultural Sciences) 2022

## ABSTRACT

In this present study, spinel nickel aluminate ( $\text{NiAl}_2\text{O}_4$ ) nanoparticles (NPs) were synthesized using *Pedaliium murex* Linn (family: *Pedaliaceae*) extract, aluminium (III) nitrate and nickel (II) nitrate as precursors. Structural and morphological properties of  $\text{NiAl}_2\text{O}_4$  NPs were determined by high resolution scanning electron microscopy (HR-SEM), high resolution transmission electron microscopy (HR-TEM), powder X-ray diffraction (PXRD), vibrating sample magnetometer (VSM), and Fourier transform infra-red (FT-IR) analysis. PXRD analysis confirmed the pure phase formation of  $\text{NiAl}_2\text{O}_4$  NPs. HR-SEM and HR-TEM analysis showed sphere shaped particle like nanostructures. VSM analysis shows a hysteresis loop with superparamagnetic behaviour.

**Key words:**  $\text{NiAl}_2\text{O}_4$  NPs, *Pedaliium murex* Linn extract, Green synthesis, Magnetic properties

Spinel nickel aluminates ( $\text{NiAl}_2\text{O}_4$ ) NPs have recently been discovered to be ceramic nanoscale materials that can be used in a variety of applications. According to new research, a variety of nanomaterials can cause dye degradation [1]. Because of their nanoscale size, catalytic characteristics, surface plasmonic resonance, magnetic nature, and other qualities, these nanomaterials are used [2-4]. Ferrite magnetic NPs with the chemical formula  $\text{MAl}_2\text{O}_4$  (M = Ni, Co, Cu, etc.) [5] have piqued the interest of researchers in a variety of biological domains, including photocatalysis, hyperthermia, cell labelling and so on, in recent decades. Magnetic resonance imaging (MRI) contrast agents made of spinel ferrite NPs can be used [6-10]. In this study,  $\text{NiAl}_2\text{O}_4$  NPs were eco-friendly synthesized using *Pedaliium murex* Linn extract. The physical and chemical properties of the  $\text{NiAl}_2\text{O}_4$  NPs were determined by X-ray powder diffraction (XRD), scanning electron microscopy (SEM), transmission electron microscopy (TEM), and vibrating-sample magnetometer (VSM) analyses. The obtained results were discussed herein detail.

## MATERIALS AND METHODS

Aluminium (III) nitrate, nickel (II) nitrate (Sigma-Aldrich, 99%), and *Pedaliium murex* Linn extract were utilized for the green synthesis of  $\text{NiAl}_2\text{O}_4$  NPs. Deionized (DI) water was utilized in all stages of the synthesis. Aluminium (III)

nitrate, nickel (II) nitrate and *Pedaliium murex* Linn extract mixture is placed in the microwave oven with the 850W. The mixture was kept in a microwave oven. The final product were washed well with DI water and ethanol twice finally dried at 70°C and used for further characterizations.

### Characterization techniques

The structural characterization of  $\text{NiAl}_2\text{O}_4$  NPs were performed using Rigaku Ultima X-ray diffractometer equipped with  $\text{Cu-K}\alpha$  radiation ( $\lambda = 1.5418 \text{ \AA}$ ). The surface functional groups were analyzed by Perkin Elmer FT-IR spectrometer. Morphological studies and energy dispersive X-ray analysis (EDX) of  $\text{NiAl}_2\text{O}_4$  NPs have been performed with a Jeol JSM6360 high resolution scanning electron microscopy (HR-SEM). UV-Visible diffuse reflectance spectrum (DRS) was recorded using Cary100 UV-Visible spectrophotometer to estimate their band gap energy ( $E_g$ ). Magnetic measurements were carried out at room temperature using a PMC MicroMag 3900 model vibrating sample magnetometer equipped with 1 Tesla magnet.

## RESULTS AND DISCUSSION

### Powder XRD analysis

Figure 1 shows the powder XRD diagram of  $\text{NiAl}_2\text{O}_4$  NPs. The peaks mentioned in the XRD spectra correspond to the cubic spinel structure of the  $\text{NiAl}_2\text{O}_4$  NPs [11-13]. The crystallization degree of  $\text{NiAl}_2\text{O}_4$  NPs depends on the synthesis procedure, temperature and time. The average crystallite size of  $\text{NiAl}_2\text{O}_4$  NPs was calculated using Debye Scherrer formula given in eqn. 1:

$$L = \frac{0.89\lambda}{\beta \cos \theta} \quad \text{---- (1)}$$

\* A. Manikandan

✉ manikandan.research@bharathuniv.ac.in

<sup>1-2</sup> Department of Chemistry, Bharath Institute of Higher Education and Research (BIHER), Chennai - 600 073, Tamil Nadu, India

where  $L$  is the crystallite size,  $\lambda$ , the X-ray wavelength,  $\theta$ , the Bragg diffraction angle and  $\beta$ , the full width at half maximum

(FWHM). The average crystallite size ' $L$ ' calculated from the diffraction peaks was found to be around 18 nm.

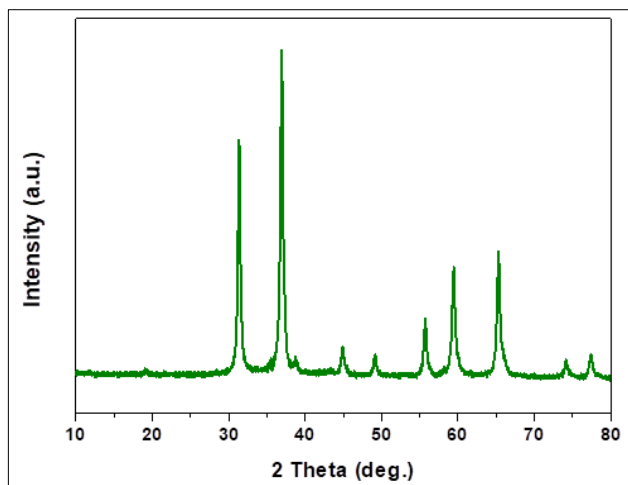


Fig 1 XRD analysis of NiAl<sub>2</sub>O<sub>4</sub> NPs

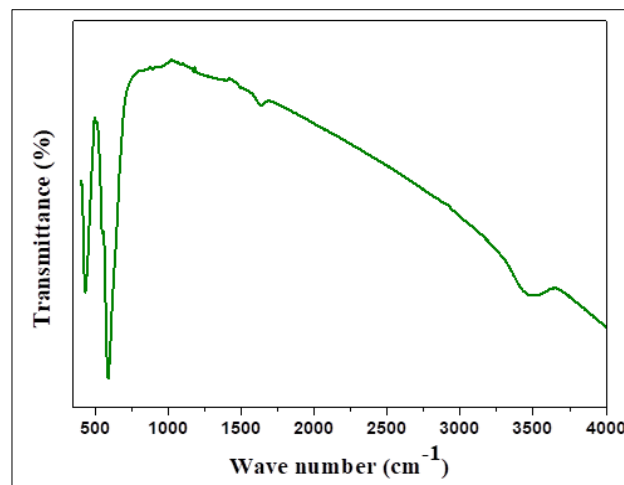


Fig 2 FT-IR spectra of NiAl<sub>2</sub>O<sub>4</sub> NPs

#### FT-IR analysis

Fourier change infrared spectra (FTIR) of spinel NiAl<sub>2</sub>O<sub>4</sub> NPs are shown in Fig. 2. The band around 435 – 750 cm<sup>-1</sup> shows the formation of spinel NiAl<sub>2</sub>O<sub>4</sub> NPs. A band at 525 cm<sup>-1</sup> is distinguished for Al-O and Ni-O. The wave number of 3435 cm<sup>-1</sup> is more ingestion band is noticed H<sub>2</sub>O molecules [22]. The bowing methods of O-H band are seen in roughly 1622 cm<sup>-1</sup>.

#### UV-Visible spectral analysis

The band gap energy ( $E_g$ ) of NiAl<sub>2</sub>O<sub>4</sub> NPs can be evaluated using the Kubelka - Munk model. UV-Vis. diffuse reflectance (UV-DRS) spectra of NiAl<sub>2</sub>O<sub>4</sub> NPs were shown in Fig. 3 and the band gap energy  $E_g$  2.47, indicating that NiAl<sub>2</sub>O<sub>4</sub>

NPs exhibited an intense absorption in the visible range [16-18]. DRS analysis was used to study the relation of crystallite size and band gap of the semiconductors. Kubelka-Munk function,  $F(R)$  is directly proportional to the absorption coefficient ( $\alpha$ ) and the value is estimated from the following eqn. 2,

$$(F(R)) = \alpha = \frac{(1-R)^2}{2R} \quad \text{---- (2)}$$

where,  $F(R)$  is Kubelka-Munk function,  $\alpha$ , the absorbance,  $R$ , the reflectance. A graph is plotted between  $[F(R)h\nu]^2$  and  $h\nu$ , the obtained intercept value is the  $E_g$  of the NiAl<sub>2</sub>O<sub>4</sub> NPs. The estimated  $E_g$  of NiAl<sub>2</sub>O<sub>4</sub> NPs is 2.47 eV.

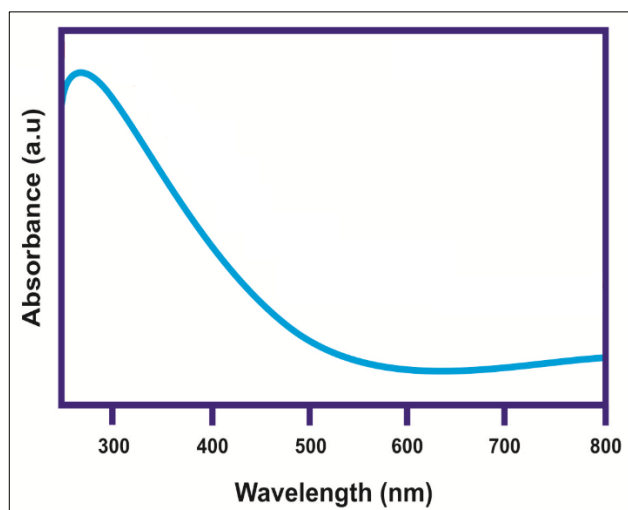


Fig 3 UV-Vis absorption spectra of NiAl<sub>2</sub>O<sub>4</sub> NPs

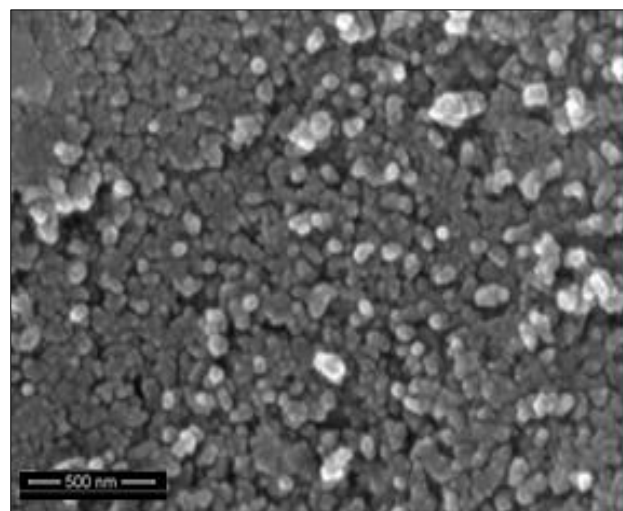


Fig 4 SEM image of NiAl<sub>2</sub>O<sub>4</sub> NPs

#### SEM analysis

Figure 4 shows HR-SEM images of NiFe<sub>2</sub>O<sub>4</sub> NPs prepared by *Petalium murex* Linn extract assisted microwave combustion method. HR-SEM images of the NiAl<sub>2</sub>O<sub>4</sub> NPs confirmed the nanostructured spherical shaped surface morphology of the products with 14 to 18 nm sizes of the NPs, which are crystallized well in a short time by the microwave heating route.

#### TEM analysis

HR-TEM image of NiAl<sub>2</sub>O<sub>4</sub> NPs are exposed in Fig. 5a. HR-TEM images confirmed the prepared particles are well formed and are in nano regime. The micrographs establish the reasonable uniformity of the particle in size and shape without any agglomeration and particle size around 12-18 nm, which is in close agreement with XRD crystallite size. SAED pattern of NiAl<sub>2</sub>O<sub>4</sub> NPs are as shown in Fig. 5b. Several concentric rings in the figure suggest that the as prepared material is well crystalline in nature.

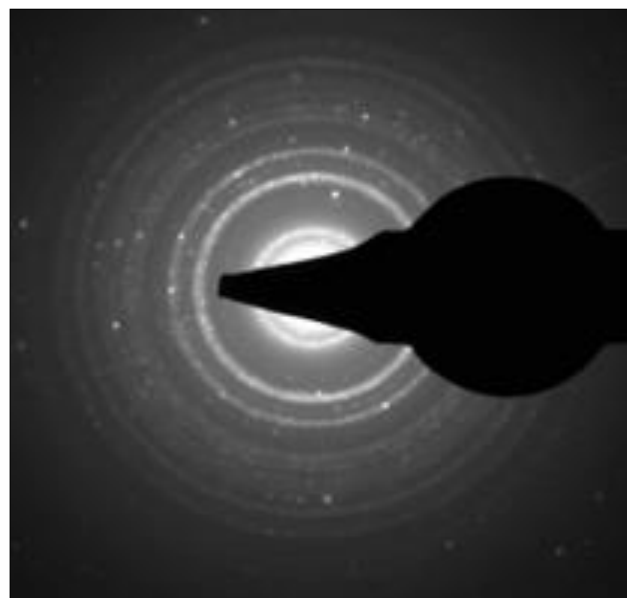
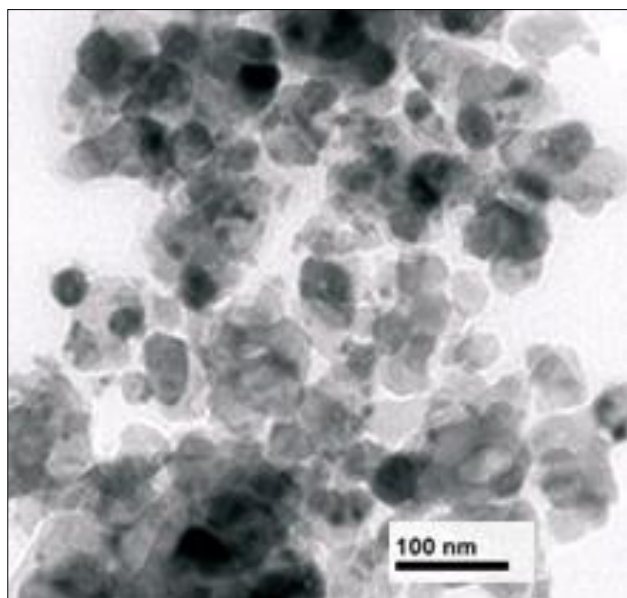


Fig 5 TEM image (a) and SAED pattern (b) of  $\text{NiAl}_2\text{O}_4$  NPs

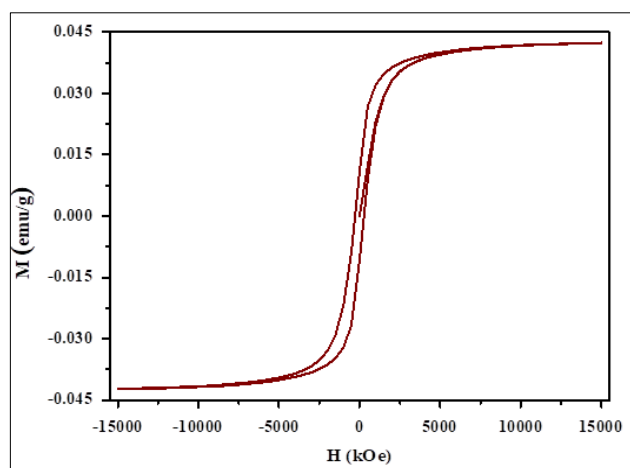


Fig 6 VSM results of  $\text{NiAl}_2\text{O}_4$  NPs

of  $M_s$  of  $\text{NiAl}_2\text{O}_4$  NPs depends on their size, crystallinity and structure [22–25]. The spinel structure and superparamagnetic behaviour of spinel  $\text{NiAl}_2\text{O}_4$  NPs were confirmed by XRD and VSM analyses.

## CONCLUSION

Spinel nickel aluminate ( $\text{NiAl}_2\text{O}_4$ ) nanoparticles (NPs) were synthesized using *Pedaliaceae* extract, aluminium (III) nitrate and nickel (II) nitrate as precursors. Structural and morphological properties of  $\text{NiAl}_2\text{O}_4$  NPs were determined by HR-SEM, HR-TEM, XRD, VSM, and FT-IR analysis. XRD analysis confirmed the pure phase formation of spinel  $\text{NiAl}_2\text{O}_4$  NPs. HR-SEM and HR-TEM analysis showed sphere shaped particle like nanostructures. VSM analysis recorded at room temperature shows a hysteresis loop with superparamagnetic behaviour.

## Acknowledgment

The authors are thankful to Tamil Nadu State Council for Science and Technology (TNSCST), DOTE Campus, Chennai for the financial support (S&T Project: TNSCST/ STP-PRG/AR/2018-2019/9307).

## VSM analysis

The magnetic properties of spinel  $\text{NiAl}_2\text{O}_4$  NPs at  $\pm 15\text{kOe}$  applied field are shown in Figure 5. The amount of magnetic saturation ( $M_s$ ) for the synthesized  $\text{NiAl}_2\text{O}_4$  NPs was  $4.256 \times 10^{-2}$  emu/g. The obtained result shows superparamagnetic in nature [19–21]. Additionally, the amount

## LITERATURE CITED

1. A. Manikandan, R. Sridhar, S. A. Antony, S. Ramakrishna, A simple aloe vera plant-extracted microwave and conventional combustion synthesis: Morphological, optical and catalytic properties of magnetic  $\text{CoFe}_2\text{O}_4$  nanostructures, J. Mol. Struct., 1076 (2014) 188–200.
2. N. Babitha, L. Srimathi Priya, S. Rosy Christy, A. Manikandan, A. Dinesh, M. Durka, and S. Arunadevi, Enhanced Antibacterial Activity and Photo-Catalytic Properties of  $\text{ZnO}$  Nanoparticles: *Pedaliaceae* Plant Extract-Assisted Synthesis, J. Nanosci. Nanotech. 19 (2019) 2888–2894.
3. K. Chitra, A. Manikandan, S. Arul Antony, Effect of poloxamer on *Zingiber officinale* extracted green synthesis and antibacterial studies of silver nanoparticles, J. Nanosci. Nanotech. 16 (2016) 758–764.
4. A. Manikandan, M. Durka, S. Arul Antony, *Hibiscus rosa-sinensis* leaf extracted green methods, magneto-optical and catalytic properties of spinel  $\text{CuFe}_2\text{O}_4$  nano- and microstructures, J. Inorg. Organomet. Polym., 25 (2015) 1019–1031.
5. K. Chitra, K. Reena, A. Manikandan, S. Arul Antony, Antibacterial studies and effect of poloxamer on gold nanoparticles by *Zingiber officinale* extracted green synthesis, J. Nanosci. Nanotech. 15 (2015) 4984–4991.
6. C. Sambathkumar, V. Manirathinam, A. Manikandan, M. Krishna Kumar, S. Sudhakar, P. Devendran, Solvothermal synthesis of  $\text{Bi}_2\text{S}_3$  nanoparticles for active photocatalytic and energy storage device applications, J. Mater. Sci. Mater. Elect., 32 (2021) 20827–20843.
7. SP Ratnayake, M Mantilaka, C Sandaruwan, D Dahanayake, E Murugan, Carbon quantum dots-decorated nano-zirconia: a highly efficient photocatalyst, Applied Catalysis A: General, 2019, 570, 23–30.

8. E Murugan, I Pakrudheen, Efficient amphiphilic poly (propylene imine) dendrimer encapsulated ruthenium nanoparticles for sensing and catalysis applications, *Science of Advanced Materials*, 2015, 7 (5), 891-901.
9. E Murugan, JN Jebaranjitham, A Usha Synthesis of polymer-supported dendritic palladium nanoparticle catalysts for Suzuki coupling reaction, *Applied Nanoscience*, 2012, 2 (3), 211-222
10. E Murugan, SS Kumar, KM Reshna, S Govindaraju, Highly sensitive, stable g-CN decorated with AgNPs for SERS sensing of toluidine blue and catalytic reduction of crystal violet, *Journal of Materials Science* 2019, 54 (7), 5294-5310
11. E Murugan, S Santhoshkumar, S Govindaraju, M Palanichamy, Silver nanoparticles decorated g-C3N4: An efficient SERS substrate for monitoring catalytic reduction and selective Hg<sup>2+</sup> ions detection, *Spectrochimica Acta Part A: Molecular and Biomolecular Spectroscopy*, 2021, 246, 119036.
12. E Murugan, R Rangasamy, Development of stable pollution free TiO<sub>2</sub>/Au nanoparticle immobilized green photo catalyst for degradation of methyl orange, *Journal of Biomedical Nanotechnology*, 2011, 7 (1), 225-228.
13. K. Chitra, A. Manikandan, S. Moortheswaran, K. Reena, S. Arul Antony, Zingiber officinale extracted green synthesis of copper nanoparticles: Structural, morphological and antibacterial studies, *Adv. Sci. Eng. Med.*, 7 (2015) 710-716.
14. A. Manikandan, M. Durka, M. A. Selvi, S. Arul Antony, Sesamum indicum plant extracted microwave combustion synthesis and opto-magnetic properties of spinel Mn<sub>x</sub>Co<sub>1-x</sub>Al<sub>2</sub>O<sub>4</sub> nano-catalysts, *J. Nanoscience. Nanotech.* 16 (2016) 448-456.
15. A. Manikandan, M. Durka, M. A. Selvi, S. Arul Antony, Aloe vera plant extracted green synthesis, structural and opto-magnetic characterizations of spinel Co<sub>x</sub>Zn<sub>1-x</sub>Al<sub>2</sub>O<sub>4</sub> nano-catalysts, *J. Nanoscience. Nanotech.* 16 (2016) 357-373.
16. P. Bhavani, A. Manikandan, P. Paulraj, A. Dinesh, M. Durka, and S. Arul Antony, Okra (*Abelmoschus esculentus*) Plant Extract-Assisted Combustion Synthesis and Characterization Studies of Spinel ZnAl<sub>2</sub>O<sub>4</sub> Nano-Catalysts, *J. Nanoscience. Nanotech.* 18 (2018) 4072–4081.
17. D. Maruthamani, S. Vadivel, M. Kumaravel, B. Saravanakumar, B. Paul, S. Sankar Dhar, A. H. Yangjeh, A. Manikandan, G. Ramadoss, Facile synthesis of Bi<sub>2</sub>O<sub>3</sub>/reduced graphene oxide (RGO) nanocomposite for supercapacitor and visible light photocatalytic applications, *J. Colloid Interf. Sci.*, 498 (2017) 449-459.
18. A. Shameem, P. Devendran, V. Siva, M. Raja, A. Manikandan, S. A. Bahadur, Preparation and characterization studies of nanostructured CdO thin films by SILAR method for photocatalytic applications, *J. Inorg. Organomet. Polym.*, 27 (2017) 692–699.
19. A. Silambarasu, A. Manikandan, K. Balakrishnan, Room temperature superparamagnetism and enhanced photocatalytic activity of magnetically reusable spinel ZnFe<sub>2</sub>O<sub>4</sub> nano-catalysts, *J. Supercond. Nov. Magn.*, 30 (2017) 2631–2640.
20. R. Bomila, S. Srinivasan, S. Gunasekaran, A. Manikandan, Enhanced photocatalytic degradation of methylene blue dye, opto-magnetic and antibacterial behaviour of pure and La-doped ZnO nanoparticles, *J. Supercond. Nov. Magn.*, 31 (2018) 855–864.
21. I. J. C. Lynda, M. Durka, A. Dinesh, A. Manikandan, S. K. Jaganathan, A. Baykal, S. Arul Antony, Enhanced Magneto-optical and Photocatalytic Properties of Ferromagnetic Mg<sub>1-y</sub>Ni<sub>y</sub>Fe<sub>2</sub>O<sub>4</sub> (0.0 ≤ y ≤ 1.0) Spinel Nano-ferrites, *J. Supercond. Nov. Magn.*, 31 (2018) 3637–3647.
22. S. Velanganni, A. Manikandan, J. Joseph Prince, C. Neela Mohan, R. Thiruneelakandan, Nanostructured ZnO coated Bi<sub>2</sub>S<sub>3</sub> thin films: Enhanced photocatalytic degradation of Methylene blue dye, *Physica B*, 545 (2018) 383-389.
23. J. A. H. Sheela, S. Lakshmanan, A. Manikandan, S. A. Antony, Structural, morphological and optical properties of ZnO, ZnO:Ni<sup>2+</sup> and ZnO:Co<sup>2+</sup> nanostructures by hydrothermal process and their photocatalytic activity, *J. Inorg. Organomet. Polym.* 28 (2018) 2388–2398.
24. R. A. Senthil, S. Osman, J. Pan, Y. Sun, T. R. Kumar, A. Manikandan, A facile hydrothermal synthesis of visible-light responsive BiFeWO<sub>6</sub>/MoS<sub>2</sub> composite as superior photocatalyst for degradation of organic pollutants, *Ceram. Int.*, 45 (2019) 18683-18690.
25. R. A. Senthil, S. Osman, J. Pan, A. Khan, V. Yang, T. R. Kumar, Y. Sun, A. Manikandan, One-pot preparation of AgBr/α-Ag<sub>2</sub>WO<sub>4</sub> composites with superior photocatalytic activity under visible-light irradiation, *Colloids and Surf. A: Physicochem. Eng. Aspects*, 586 (2020) 124079.
26. S. Rathinavel, R. Deepika, D. Panda, A. Manikandan, Synthesis and characterization of MgFe<sub>2</sub>O<sub>4</sub> and MgFe<sub>2</sub>O<sub>4</sub>/rGO nanocomposites for the photocatalytic degradation of methylene blue, *Inorg. Nano-Metal Chem.*, 51, 2 (2021) 210-217.
27. A Muthukrishnaraj, SS Kalaivani, A Manikandan, Helen P Kavitha, R Srinivasan, N Balasubramanian, Sonochemical synthesis and visible light induced photocatalytic property of reduced graphene oxide@ ZnO hexagonal hollow rod nanocomposite, *J. Alloys Compds.*, 83625 (2020) 155377.
28. T. L. Ajeesha, A. Ashwini, Mary George, A. Manikandan, J. Arul Mary, Y. Slimani, M. A. Almessiere, A. Baykal, Nickel substituted MgFe<sub>2</sub>O<sub>4</sub> nanoparticles via co-precipitation method for photocatalytic applications, *Physica B*, 606 (2021) 412660.
29. R. Renuga, A. Manikandan, J. A. Mary, A. Muthukrishnaraj, A. Khan, S. Srinivasan, B. Abdullah M. Al Alwan and K. M. Khedher, Enhanced Magneto-Optical, Morphological, and Photocatalytic Properties of Nickel-Substituted SnO<sub>2</sub> Nanoparticles, *J. Supercond. Nov. Magn.*, 34 (2021) 825–836.
30. M. George, T.L. Ajeesha, A. Manikandan, Ashwini Anantharaman, R.S. Jansi, E. Ranjith Kumar, Y. Slimani, M.A. Almessiere, A. Baykal, Evaluation of Cu-MgFe<sub>2</sub>O<sub>4</sub> spinel nanoparticles for photocatalytic and antimicrobial activities, *J. Phys. Chem. Solids*, 153 (2021) 110010.
31. K. Geetha, R. Udhayakumar, A. Manikandan, Enhanced magnetic and photocatalytic characteristics of cerium substituted spinel MgFe<sub>2</sub>O<sub>4</sub> ferrite nanoparticles, *Physica B*, 615 (2021) 413083.